Journal of Catalysis 279 (2011) 1–11

Contents lists available at ScienceDirect

Journal of Catalysis

journal homepage: www.elsevier.com/locate/jcat

Microwave-assisted synthesis of palladium nanoparticles supported on graphene: A highly active and recyclable catalyst for carbon–carbon cross-coupling reactions

Ali R. Siamaki [b,a], Abd El Rahman S. Khder [a], Victor Abdelsayed [a], M. Samy El-Shall [a,b,*], B. Frank Gupton [b,a,*]

[a] Department of Chemistry, Virginia Commonwealth University, Richmond, VA 23284, United States
[b] Department of Chemical Engineering, Virginia Commonwealth University, Richmond, VA 23284, United States

ARTICLE INFO

Article history:
Received 30 August 2010
Revised 5 December 2010
Accepted 6 December 2010
Available online 26 January 2011

Keywords:
Heterogeneous catalysis
Graphene
Palladium nanoparticles
Cross-coupling reactions
Suzuki coupling
Heck cross-coupling

ABSTRACT

We have developed an efficient method to generate highly active Pd nanoparticles supported on graphene (Pd/G) by microwave-assisted chemical reduction of the corresponding aqueous mixture of a palladium salt and dispersed graphite oxide (GO) sheets. The Pd/G demonstrated excellent catalytic activity for the carbon–carbon cross-coupling reactions (Suzuki, and Heck) with a broad range of utility under ligand-free ambient conditions in an environmentally friendly solvent system. It also offers a remarkable turnover frequency (108,000 h^{-1}) observed in the microwave-assisted Suzuki cross-coupling reactions with easy removal from the reaction mixture, recyclability with no loss of activity, and significantly better performance than the well-known commercial Pd/C catalyst. The catalyst was fully characterized by a variety of spectroscopic techniques including X-ray diffraction (XRD), Raman, TGA, electron microscopy (SEM, TEM), and X-ray photoelectron spectroscopy (XPS). The remarkable reactivity of the Pd/G catalyst toward Suzuki cross-coupling reactions is attributed to the high degree of the dispersion and concentration of Pd(0) nanoparticles supported on graphene sheets with small particle size of 7–9 nm due to an efficient microwave-assisted reduction method.

1. Introduction

Graphene's unique hexagonal atomic layer structure and unusual properties, including the highest electron mobility of all known materials at room temperature, has motivated the development of new composite materials for nanoelectronics, supercapacitors, batteries, photovoltaics, and related devices [1–11]. However, other properties of graphene such as high thermal, chemical, and mechanical stability as well as high surface area also represent desirable characteristics as 2D support layers for metallic and bimetallic nanoparticles in heterogeneous catalysis, fuel cells, chemical sensors, and hydrogen storage applications [12–23].

Recent advances in the production of graphene sheets through the reduction of exfoliated graphite oxide (GO) have provided efficient approaches for the large-scale production of chemically converted graphene (CCG) sheets, which can be readily used as a catalyst support [24–28]. One of the catalytic applications in which graphene support may provide some significant advantages is in the area of cross-coupling chemistry [29,30]. Palladium-catalyzed cross-coupling reactions have been of strategic importance in organic synthesis since their discovery in the 1970s [29–33]. These reactions have been extensively used for the assembly of complex organic molecules for a wide variety of applications with considerable impact on the chemical and pharmaceutical industries [29–33]. Due to their broad applicability for C–C bond formation, enormous interest continues in this area with more focus directed toward developing more efficient and recyclable catalysts that allow for industrial applications within environmentally benign processes.

Cross-coupling reactions have typically been performed under homogeneous conditions employing a ligand to enhance the catalytic activity and selectivity for specific reactions [29–33]. However, the issues associated with homogeneous catalysis remain a challenge to pharmaceutical applications of these synthetic tools due to the lack of recyclability and potential contamination from residual metals in the reaction product [34,35]. In order to address this issue, a significant effort has been made to advance the development of cross-coupling catalysts where the palladium is fixed to a solid support such as activated carbon [36,37], zeolites [38,39], polymers [40,41], or nanoparticles [42–46]. Although heterogeneous supports allow efficient recycling, a decrease in the activity of the immobilized catalysts is frequently observed [47,48]. Therefore, the development of heterogeneous Pd nanocatalysts that combine high activity, stability, and recyclability is an important goal of nanomaterials research that is likely to have a considerable impact on the chemical and pharmaceutical industries in the future.

* Corresponding authors. Address: Department of Chemistry, Virginia Commonwealth University, Richmond, VA 23284, United States.
E-mail addresses: mselshal@vcu.edu (M.S. El-Shall), bfgupton@vcu.edu (B.F. Gupton).

0021-9517/$ - see front matter © 2010 Elsevier Inc. All rights reserved.
doi:10.1016/j.jcat.2010.12.003

Only recently have graphene (G) and graphite oxide (GO) been considered as potential support systems for palladium-catalyzed C–C coupling applications [49]. Because of the higher specific surface area (1500 m^2/g, theoretical value 2600 m^2/g)[2] and thermal stability of graphene when compared to graphite oxide (surface area 200–400 m^2/g), G-based nanocatalysts might be expected to exhibit superior activity compared to GO-based catalysts [5,6]. We hypothesized that the preparation of these materials may play a critical role in the catalytic activity for specific synthetic applications. For this reason, we chose to evaluate the cross-coupling activity of Pd/G nanomaterials prepared by a procedure developed in our group. In this paper, we report on the excellent catalytic activity and stability of palladium nanoparticles supported on graphene (Pd/G) as a catalyst for both Suzuki and Heck C–C coupling reactions. Furthermore, we have obtained valuable insights from X-ray photoelectron spectroscopy (XPS) studies into the critical parameters that affect heterogeneous cross-coupling catalytic activity in these specific applications. We hope that this work provides a significant step toward the development of clean technologies for organic synthesis.

In the present work, the Pd/G nanocatalysts were prepared using the recently reported microwave irradiation (MWI) method [28]. MWI has been demonstrated for the synthesis of a variety of nanomaterials including metals, metal oxides, bimetallic alloys, and semiconductors with controlled size and shape without the need for high temperature or high pressure [50–54]. The main advantage of MWI over other conventional heating methods is that the reaction mixture is heated uniformly and rapidly. This has been demonstrated for the acceleration of homogeneous catalysis in organic synthesis [55]. Due to the difference in the solvent and reactant dielectric constants, selective dielectric heating can provide significant enhancement in the transfer of energy directly to the reactants, which causes an instantaneous internal temperature rise [55]. This temperature rise in the presence of hydrazine hydrate as a reducing agent has provided a facile and efficient method by which palladium ions and GO can be effectively reduced into a dispersion of metallic nanoparticles supported on the large surface area of the graphene sheets. The reduction of GO by hydrazine hydrate under MWI proceeds by rapid deoxygenation of GO to create C–C and C=C bonds [24–28]. Unlike conventional thermal heating, MWI allows better control of the extent of GO reduction by hydrazine hydrates as both the MWI power and time can be adjusted to yield a nearly complete concurrent reduction of GO and the palladium salt. In contrast, the corresponding palladium supported on graphite oxide sheets (Pd/GO) catalyst was prepared by the microwave-assisted deposition of palladium nitrate in a GO dispersion without the addition of hydrazine hydrate. In this case, the temperature rise during MWI causes subsequent supersaturation and nucleation to form Pd nanoparticles supported on the GO sheets.

2. Experimental

2.1. Materials and methods

High-purity graphite powder (99.9999%, 200 mesh) was purchased from Alfa Aesar. Palladium nitrate (10 wt.% in 10 wt.% HNO_3, 99.999%) and hydrazine hydrate were obtained from Sigma Aldrich. Aryl bromide and chloride, potassium carbonate, aryl-substituted boronic acid, and olefins were also purchased from Aldrich and used as received. A mixture of ethanol/deionized water was used for the Suzuki and Heck cross-coupling reactions.

TEM images were obtained using a JEOL JEM-1230 electron microscope operated at 120 kV equipped with a Gatan UltraScan 4000SP 4 K × 4 K CCD camera. Samples for TEM were prepared by placing a droplet of a colloid suspension in toluene on a Formvar carbon-coated, 300-mesh copper grid (Ted Pella) and allowed to evaporate in air at room temperature. The small-angle X-ray diffraction (SA-XRD) patterns were measured at room temperature with an X'Pert Philips Materials Research Diffractometer using the Cu KαR radiation. Scanning electron microscopy (SEM) and energy-dispersive X-ray spectroscopy (EDS) were carried out using a Quantum DS-130S Dual Stage Electron Microscope. The morphology of the graphene sheets was examined by an atomic force microscope (Nano-Scope IIIa, Digital Instruments) using tapping mode. The thermal gravimetric analysis was carried out on a TGA Q5000 from TA instruments. The Raman spectra were measured using an excitation wavelength of 457.9 nm provided by a Spectra-Physics model 2025 argon ion laser. The laser beam was focused to a 0.10-mm-diameter spot on the sample with a laser power of 1 mW. The samples were pressed into a depression at the end of a 3-mm-diameter stainless steel rod, held at a 30 degree angle in the path of the laser beam. The detector was a Princeton Instruments 1340 × 400 liquid nitrogen CCD detector, attached to a Spex model 1870 0.5 meter single spectrograph with interchangeable 1200 and 600 lines/mm holographic gratings (Jobin–Yvon). The Raman scattered light was collected by a Canon 50 mm f/0.95 camera lens. Though the holographic gratings provided high discrimination, Schott and Corning glass cut-off filters were used to provide additional filtering of reflected laser light, when necessary. The X-ray photoelectron spectroscopy (XPS) analysis was performed on a Thermo Fisher Scientific ESCALAB 250 using a monochromatic Al KR X-ray. GC–MS analyses were performed on Agilent 6890 gas chromatograph equipped with an Agilent 5973 mass selective detector. A CEM Discover microwave instrument was used for cross-coupling reactions. The reactions were performed at operator selectable power output of 250 W. ^1H and ^{13}C NMR were acquired on a Mercury 300 MHz spectrometer. High-resolution mass spectrometry analyses were obtained from the Virginia Commonwealth University mass spectrometry facilities.

2.2. Synthesis of Pd/G and Pd/GO nanoparticles

In the experiments, GO was prepared by the oxidation of high-purity graphite powder (99.9999%, 200 mesh) with $H_2SO_4/KMnO_4$ according to the method of Hummers and Offeman [56]. After repeated washing of the resulting yellowish-brown cake with hot water, the powder was dried at room temperature under vacuum overnight. For the preparation of Pd/G, 0.1 g of the dried GO and an appropriate amount of palladium nitrate (10 wt.% in 10 wt.% HNO_3, 99.999%) were sonicated in deionized water until a homogeneous yellow dispersion was obtained. The solution was placed inside a conventional microwave after adding 100 μl of the reducing agent hydrazine hydrate (HH). The microwave oven (Emerson MW8119SB) was then operated at full power (1000 W), 2.45 GHz, in 30-s cycles (on for 10 s, off and stirring for 20 s) for a total reaction time of 60 s. The yellow solution of Pd nitrate-GO changed to a black color, indicating the completion of the chemical reduction to graphene. The Pd/G sheets were separated by using an Eppendorf 5804 centrifuge operated at 5000 rpm for 15 min and dried overnight under vacuum. The same method was also used for the preparation of Pd/GO except that no HH was added during the MWI.

2.3. General procedure for Suzuki reactions

Aryl bromide (0.51 mmol, 1 eq.) was dissolved in a mixture of 8 mL H_2O:EtOH (1:1) and placed in a 35-mL microwave tube. To this were added the aryl boronic acid (0.61 mmol, 1.2 eq.) and potassium carbonate (1.53 mmol, 3 eq.). Palladium on graphene nanoparticles (Pd/G) (2.1 mg, 1.53 μmol, 0.3 mol%) were then

added, and the tube was sealed and heated under microwave irradiation (250 W, 2.45 MHz) at the certain temperature and time which is indicated in Table 2. Upon the completion of the reaction period, the reaction mixture was diluted with 20 mL of H_2O and extracted with CH_2Cl_2 (3×50 mL). The organic layers were combined, dried over anhydrous Na_2SO_4, and filtered. The solvent in the filtrate was then removed *in vacuo* to give a solid. The pure products were obtained by flash chromatography using hexane:ethyl acetate as the eluent or by washing the solid products with an appropriate non-polar solvent such as hexanes followed by decanting the hexanes layer.

2.4. General procedure for the Heck coupling

Aryl bromide (0.51 mmol, 1 eq.) was dissolved in a mixture of 8 mL H_2O; EtOH (1:1) and placed in a 35-mL microwave tube. To this were added the corresponding alkene (1.02 mmol, 2 eq.) and potassium carbonate (1.53 mmol, 3 eq.). Palladium on graphene nanoparticles (Pd/G) (2.1 mg, 1.53 μmol, 0.3 mol%) were then added; the tube was sealed and heated under microwave irradiation (250 W, 2.45 MHz) at 150 °C, for 10 min. Upon the completion of microwave heating, the reaction mixture was extracted with CH_2Cl_2 (3×50 mL). The organic layers were combined, dried over anhydrous Na_2SO_4, and filtered. The solvent in the filtrate was then removed *in vacuo* to give a solid. The pure products were obtained by flash chromatography using hexane:ethyl acetate as the eluent or by washing the solid products with an appropriate non-polar solvent such as hexanes followed by decanting the hexanes layer.

2.5. Procedure for recycling the catalysts

Bromobenzene (50 mg, 0.32 mmol, 1 eq.) was dissolved in a mixture of 4 mL H_2O:EtOH (1:1) and placed in a 10-mL microwave tube. To this were added phenyl boronic acid (47 mg, 0.382 mmol, 1.2 eq.) and potassium carbonate (133 mg, 0.96 mmol, 3 eq.). Palladium catalyst (1.3 mg, 0.96 μmol, 0.3 mol%) was then added; the tube was sealed and heated at 80 °C for 5 min under microwave irradiation (250 W, 2.45 MHz). The progress of the reaction was monitored by GC–MS analysis. After the completion of the reaction, the mixture was diluted with 10 mL of EtOH and shaken. The entire mixture was centrifuged and the solvent above the Pd nanoparticle catalyst was completely decanted. EtOH washing followed by centrifugation was repeated two additional times to assure the removal of all products from the catalyst surface. The Pd nanoparticle catalyst was then directly transferred to another microwave tube along with fresh reagents for the next run. This procedure was repeated for every run, and the percent conversion of product was determined by the means of GC–MS spectroscopy.

2.6. Procedure for catalyst concentration effects (Fig. 6)

Bromobenzene (50 mg, 0.32 mmol, 1 eq.) was dissolved in a mixture of 4 mL H_2O:EtOH (1:1) and placed in a 10-mL microwave tube. To this were added phenyl boronic acid (47 mg, 0.382 mmol, 1.2 eq.) and potassium carbonate (133 mg, 096 mmol, 3 eq.). Palladium catalysts nanoparticles (*X* mmol, *Y* mol% as indicated in Fig. 6), were then added, and the tube was sealed and stirred at room temperature (r.t.). An aliquot of the reaction mixtures was taken after 30, 60, 120, 180, 240, 300, and 360 min, diluted with 10 mL of CH_3CN, and injected into the GC/MS. The percent conversions of the products were then calculated based on the consumption of bromobenzene starting materials by means of GC–MS spectroscopy.

3. Results and discussion

3.1. Characterization of the Pd/G and Pd/GO nanoparticle catalysts

Characterization of the graphene samples prepared by the HH-MWI method was examined in detail using EDS, XPS, TEM, and AFM analyses, and the results are provided in Supporting Information (Figs. S1, S2 and S3, pages S9–S11). Here, we focus on the characterization and catalytic activity of the Pd/G and Pd/GO nanocatalysts.

Fig. 1a displays the XRD patterns of the initial graphite powder, the prepared GO, and the chemically converted graphene and Pd/G prepared by the HH-MWI method. The initial graphite powder shows the typical sharp diffraction peak at $2\theta = 26.7°$ with the corresponding *d*-spacing of 3.34 Å. The exfoliated GO sample shows no diffraction peaks from the parental graphite material and only a new broad peak at $2\theta = 10.9°$ with a *d*-spacing of 8.14 Å observed. This indicates that the distance between the carbon sheets has increased due to the insertion of interplaner oxygen functional groups [24–28]. After MWI of the GO in the presence of HH as the reducing agent, the XRD of the resulting graphene shows the disappearance of the 10.9° peak confirming the complete reduction of the GO sheets [24–28]. A similar XRD spectrum is observed for the Pd/G sample prepared by the simultaneous reduction of GO and palladium nitrate using HH under MWI. The very small broad peak around $2\theta = 26.7°$ in the Pd/G sample could suggest the presence of a minor component of multilayer graphene. The presence of Pd nanoparticles could enhance the interaction among a few graphene layers. However, the very weak intensity of the $2\theta = 26.7°$ peak indicates that the extent of multilayer graphene in the Pd/G sample is insignificant.

The Raman spectrum of graphene is characterized by three main features: the G mode arising from emission of zone-center optical phonons (usually observed at $\sim$1575 cm^{-1}), the D mode arising from the doubly resonant disorder-induced mode ($\sim$1350 cm^{-1}), and the symmetry-allowed 2D overtone mode ($\sim$2700 cm^{-1}) [24–28,57–59]. Fig. 2 compares the Raman spectra of graphene and Pd/G samples prepared by the HH-MWI method. The spectra of graphene and Pd/G show strong G-bands at 1571 cm^{-1} and 1580 cm^{-1}, respectively. In both cases, the G-band is redshifted from the G-band in GO (1594 cm^{-1}). However, the G-band of Pd/G is significantly broad and blueshifted with respect to graphene, which could be attributed to the presence of isolated double bonds that resonate at higher frequencies than the G-band of graphene [58,59]. The D-band in Pd/G at 1365 cm^{-1} is significantly stronger and broader than the D-band in graphene. The D-band in graphene at 1357 cm^{-1} and the D'-shoulder at 1616 cm^{-1} have been attributed to structural disorder at defect sites and finite size effects, respectively [57–59]. The intensity ratio of the D-band to the G-band is used as a measure of quality of the graphitic structures since for highly ordered pyrolitic graphite; this ratio approaches zero [57–59]. As shown in Fig. 2a, the graphene sample exhibits a weak disorder-induced D-band with the D–G intensity ratio of only 0.10–0.12, thus indicating the high quality of the graphene sheets prepared by the HH-MWI method. On the other hand, the presence of Pd nanoparticles appears to induce structural disorder and defects within the graphene sheets as indicated by the high intensity ratio (0.8) of the D- to G-bands in the Pd/G sample. These structural defects, although undesirable for electronic applications of graphene, could play an important role in enhancing the catalytic activity of the Pd/G nanocatalyst. We have also observed the high-energy second-order 2D-band of the graphene and Pd/G samples around 2720 cm^{-1} and 2730 cm^{-1}, respectively, as shown in Fig. 2b. The position and shape of the 2D peak depend on the number of graphene layers, and therefore,

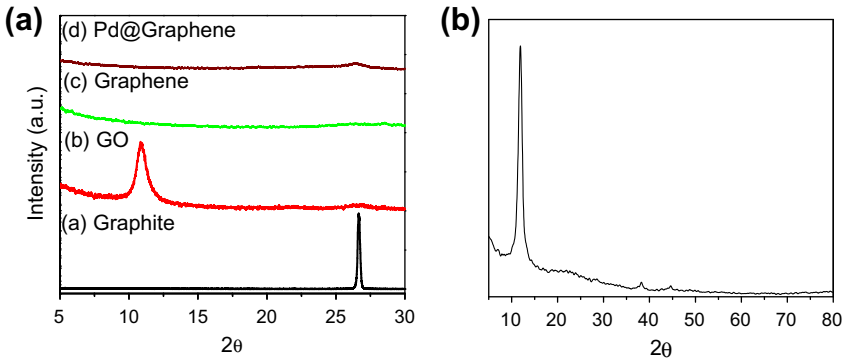

Fig. 1. (a) Small-angle XRD patterns of graphite, GO, graphene, and Pd/graphene (Pd/G) samples. (b) Small-angle XRD pattern of Pd/graphite oxide (Pd/GO) prepared by MWI of a mixture of GO and Pd nitrate solution in water without the addition of hydrazine hydrate.

the 2D peak can be used to distinguish between single-layer, bilayer, and few layer graphene (FLG) [57–59]. For example, it has been shown that sheets with more than five layers have broad 2D peaks significantly shifted to positions greater than 2700 cm^{-1} [57]. Based on these interpretations, we can estimate the number of layers in the graphene and Pd/G samples as 5–7 and 7–9, respectively.

The morphology of the Pd/G catalyst consists of platelets and extended sheets of lateral dimensions ranging from a few micrometers to tens of micrometers in length with layered structures as shown in the SEM image displayed Fig. 3a. EDS analysis (Fig. 3b) clearly shows the presence of Pd in the sample and that the sample consists mainly of carbon with an insignificant amount of oxygen probably due to the presence of some unreduced oxygen functional groups. This is consistent with the EDS and XPS spectra of the reduced GO as shown in Figs. S1 and S2, respectively (Supporting information). EDS analysis of GO before and after the hydrazine hydrate reduction under MWI shows that the oxygen content drops from 15.2% in GO to 5.2% in the chemically converted graphene, which is similar to the oxygen content measured in the Pd/G sample (Fig. 3b).

Fig. 4 displays representative TEM images of the Pd/G and Pd/GO catalysts. The palladium content in both catalysts was determined by means of inductively coupled plasma equipped with mass spectrometry (ICP-MS) and amounted to be 7.9 wt.% and 6.4 wt.%, respectively. The TEM images show the presence of uniform well-dispersed Pd nanoparticles on both G and GO sheets over very large areas of several microns as shown in Fig. S4 (Supporting information, page S12). However, the nanoparticles supported on graphene appear to be smaller than those supported on the GO sheets. From multiple samples, we can estimate the average particle sizes of the Pd nanoparticles supported on G and GO to range from 7–9 and 12–15 nm, respectively. It also appears that there is more agglomeration of the Pd nanoparticles on GO than on G. From the statistical analysis of several TEM images, the mean sizes of the Pd nanoparticles dispersed on G and GO are found to be 8 and 14 nm, respectively, consistent with the estimation of the average particle size. It should be noted that one of the important features of our catalyst preparation is the production of large graphene sheets (several microns) homogenously decorated with well-dispersed Pd nanoparticles as shown in the TEM images of Fig. S4 (Supporting information).

The XPS data of the as-prepared Pd/GO catalyst (discussed later in Section 3.4) indicate that the Pd is substantially present as Pd (II). The agglomeration of the Pd nanoparticles on GO could be enhanced by the strong interaction between the Pd ions and the oxygen functional groups of the GO. Also, the slow deposition of the Pd ions in the absence of a reducing agent during MWI could result in lower supersaturation and lower nucleation rates which result in larger particle sizes [53,54]

We have examined the thermal stability of the prepared Pd/G and Pd/GO under a nitrogen atmosphere using thermal gravimetric analysis (TGA). As shown in Fig. 5, the GO exhibits about 10% weight loss below 100 °C and more than 40% loss at 200 °C resulting from the removal of the labile oxygen-containing functional groups such as CO, CO_2, and H_2O vapors [25,28]. The Pd/GO catalyst follows very much the same thermal degradation pattern as that of GO. In contrast, G and Pd/G show much higher thermal stability with much less mass loss up to 700 °C. The mass loss in G and Pd/G is attributed to the presence of some oxygen functional groups since it is well known that although chemical reduction of GO results in removing most of the oxygen functional groups, a small amount of oxygen, mostly in the epoxy and ether groups, is always retained in the reduced GO [25–28]. The TGA data also suggest that the presence of Pd nanoparticles on the graphene sheets increases the thermal stability of the Pd/G catalyst. However, the mechanism of increasing the thermal stability of graphene by the Pd nanoparticles is not clearly explained at this point, and more research is needed in order to understand this effect.

3.2. Catalytic activity toward Suzuki reaction

3.2.1. Effect of catalyst concentration

The catalytic activity of these Pd/G and Pd/GO catalysts (with Pd contents of 7.9 wt.% and 6.4 wt.%, respectively, as determined by ICP-MS) was investigated using the Suzuki cross-coupling reaction

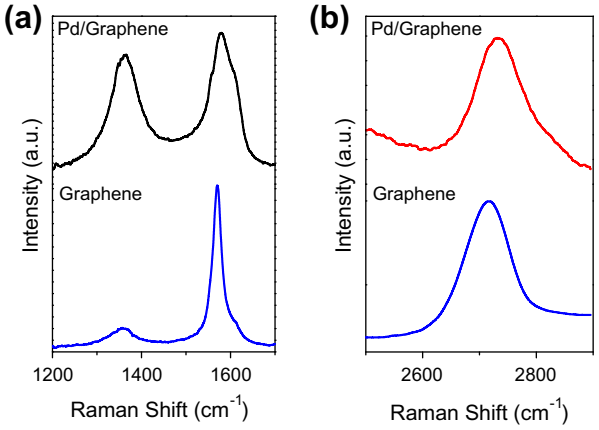

Fig. 2. (a) Raman spectra of the graphene and Pd/G samples prepared by the HH-MWI method in the G- and D-regions and (b) in the 2D-region.

of bromobenzene and phenyl boronic acid in a mixture of H_2O: EtOH (1:1) at room temperature (r.t.) (Scheme 1). Fig. 6 illustrates the % conversion of reaction in Scheme 1 for different loadings of the Pd/G and Pd/GO catalysts. While both catalysts demonstrated high activity toward Suzuki coupling, Pd/G shows slightly superior activity at lower concentrations. With 0.3 mol% loading, both catalysts show complete conversion (100%) of aryl bromide to the biphenyl product within 25 min, at room temperature (r.t.). Under the same concentration, commercially available Pd supported on activated carbon (10% Pd/C), the most often used catalyst in heterogeneous Pd-catalyzed coupling reactions, exhibits only 17% conversion after 30 min at r.t. [36,37]. In comparison, the greater catalytic activity of the Pd/G and Pd/GO over the commercial Pd/C catalyst may be attributed in part to the high level of purity of

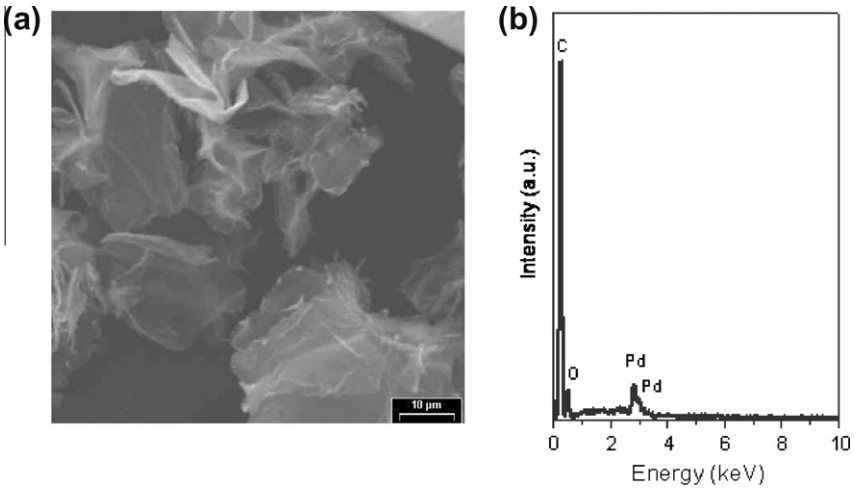

Fig. 3. (a) SEM image and (b) EDS analysis of Pd/G prepared by the HH-MWI method.

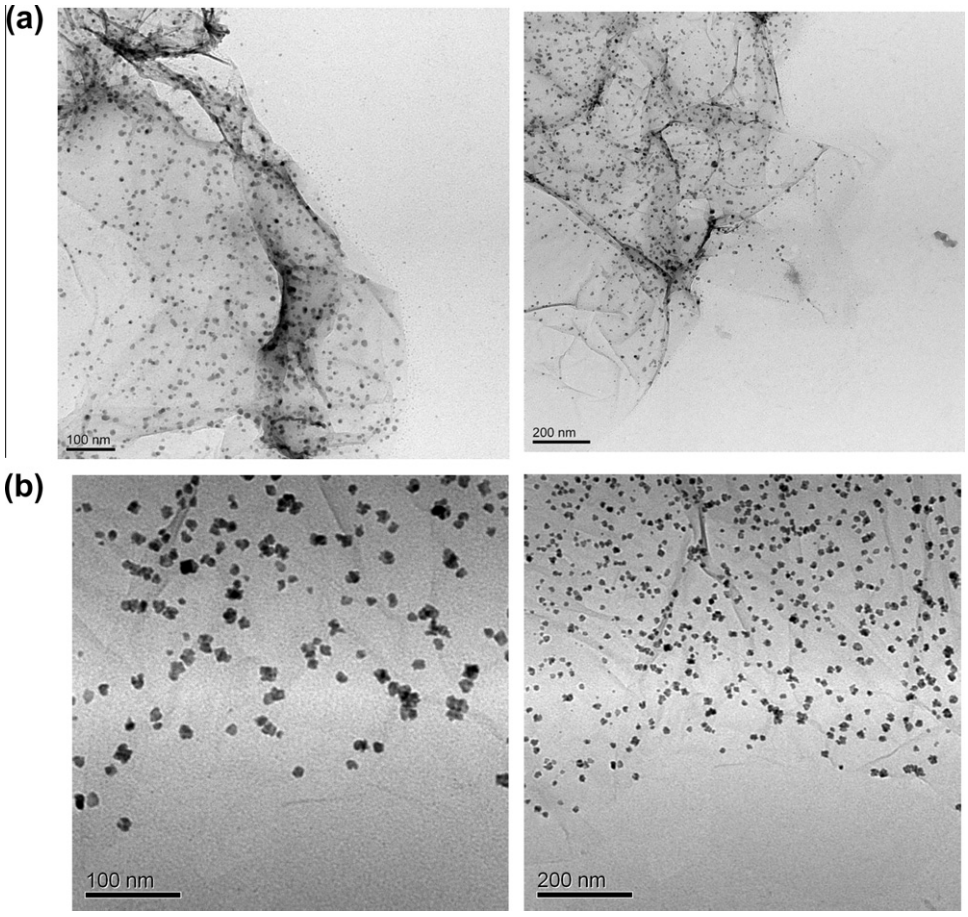

Fig. 4. TEM images of (a) 7.9 wt.% Pd/G and (b) 6.4 wt.% Pd/GO prepared by MWI of a mixture of graphite oxide (GO) and palladium nitrate in the presence and absence of hydrazine hydrate, respectively.

the starting graphite oxide support. In addition, TEM images of the commercially available Pd/C sample exhibit uneven size distributions of Pd nanoparticles within the catalyst with significant amounts of Pd agglomeration on the surface of the carbon support as shown in Fig. S5 (Supporting information).

At lower catalyst loading of 0.1 mol%, Pd/G yields the product with 100% conversion after 2.5 h, in comparison with 95% with Pd/GO. Similarly, when 0.02 mol% loading was used, both catalysts still worked effectively, giving a conversion of 97% for Pd/G and 92% for Pd/GO after 4 h. However, further reducing the concentrations provided some insight into the relative reactivity of these two catalysts. With the lowest loading of 0.007 mol%, the reaction was completed after 5 h with Pd/G at r.t. affording a yield of 94% of product, whereas the Pd/GO displayed only 72% conversion under these conditions. Interestingly, at this low concentration, Pd/G is capable of converting 63% of the bromobenzene to the biphenyl product at 80 °C under microwave heating for 5 min. Following this reaction under the same conditions (80 °C, MWI) led to 95% formation of product after 10 min. These results demonstrate the remarkable catalytic activity of Pd/G with a turnover number (TON) of 9000 and turnover frequency (TOF) of 108,000 h^{-1} (0.007 mol% Pd/G, 63% conversion at 80 °C under microwave heating for 5 min). To our knowledge, this is one of the highest turnover frequency (TOF) observed in a microwave-assisted Suzuki cross-coupling reaction by a Pd nanoparticles catalyst.

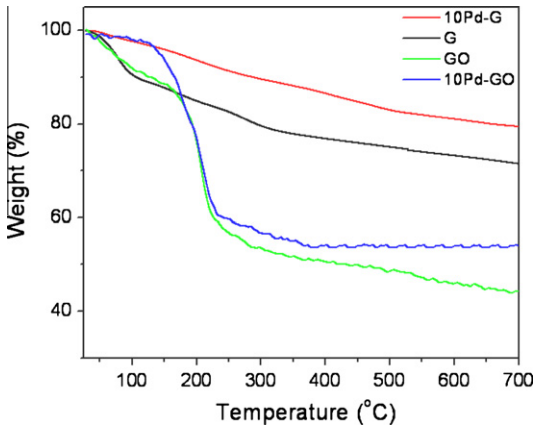

Fig. 5. Comparison of the TGA plots of graphite oxide (GO), graphene (G), and Pd/GO and Pd/G catalysts.

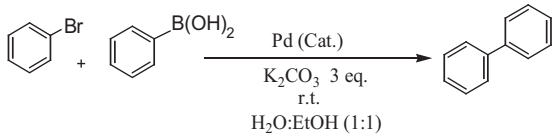

Scheme 1. Suzuki cross-coupling reaction with Pd/G and Pd/GO.

3.2.2. Recycling the Pd/G and Pd/GO catalysts

A significant practical application of heterogeneous catalysis is in the ability to easily remove the catalyst from the reaction mixture and reuse it for subsequent reactions until the catalyst is sufficiently deactivated. Thus, the ability to recycle the Pd/G and Pd/GO catalysts was studied for the Suzuki cross-coupling reaction of aryl bromide with phenyl boronic acid (Scheme 1) utilizing 0.3 mol% of these catalysts at 80 °C for 5 min using microwave irradiation as the heating source. After each reaction, the catalyst was recovered by simple washing with EtOH followed by decantation and re-used in a subsequent run. As shown in Table 1, the Pd/G nanoparticles can be easily recycled for eight times achieving a quantitative yield of the product. The activity of the catalyst dropped in runs 9 and 10, showing only 62% and 28% conversions, respectively. Evidence for deactivation of the Pd/G catalyst can be obtained from the TEM image (Fig. 7a) after the 10th run, which clearly demonstrates the agglomeration and accumulation of the Pd nanoparticles on the surface of graphene. This result indicates

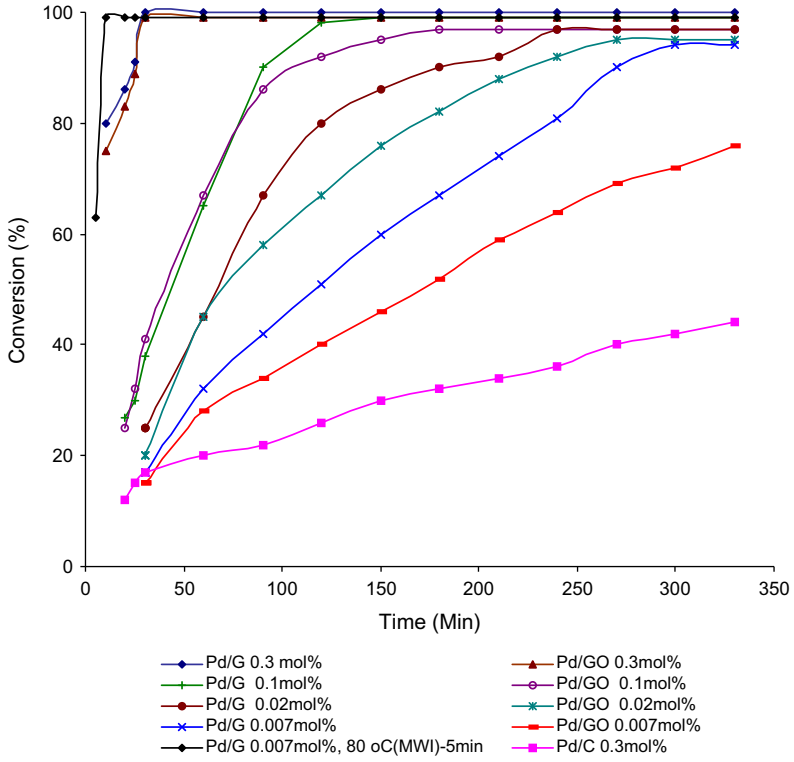

Fig. 6. Effect of catalyst concentrations for the Pd/G and Pd/GO on the conversion of reaction (Scheme 1).

that the mechanism of deactivation of the catalyst is likely to involve the formation of aggregated Pd nanoparticles which leads to the decrease in the surface area and saturation of the coordination sites. After completion of the recycling experiments, the Pd/G was separated from the reaction mixture. The reaction solution was analyzed by ICP-MS, and the palladium content in the solution was determined to be 300 ppb. Such a small amount of leached palladium may argue against complete heterogeneity of the catalytic system in this reaction. However, further evidence on the nature of the catalytic mechanism is the failure to observe reactivity after the removal of the supported nanoparticles from the reaction medium. Thus, these results provide consistent implication for the proposed release and re-deposition mechanism [60–63] by which a small quantity of Pd leaches into the reaction solution catalyzes the reaction [62,63] and re-deposits to the surface of the graphene support at the end of the reaction. In this case, the large surface area created by the support can effectively facilitate both the Pd leaching into the solution to catalyze the reaction and the re-deposition of the leached Pd on the surface of the support after the reaction is completed.

Similarly, the recyclability of Pd/GO was also examined using the same microwave-assisted Suzuki cross-coupling reaction conditions at 80 °C for 5 min (Table 1). In this case, full conversions were obtained in the runs 1–4. The activity slightly dropped in the fifth run yielding 96% conversion. The catalytic activity was further dropped in runs 6 and 7 to 54% and 23% conversions, respectively. Significant amounts of agglomeration of Pd nanoparticles on graphite oxide sheets can be observed on the TEM image prepared after the 7th run (Fig. 7b), indicating the possible deactivation pathway. Analysis of the reaction mixture by ICP-MS after the 7th run also displayed a very low palladium leaching of 350 ppb.

3.2.3. Activity of Pd/G catalyst for the preparation of other biphenyl products

To generalize the above results, the range of catalytic utility in Suzuki cross-coupling reactions for the preparation of other biphenyl products containing a broader range of functionality was investigated. For these experiments, we chose to use the Pd/G catalyst exclusively due to the superior catalytic activity demonstrated in our prior studies. As illustrated in Table 2, the Suzuki coupling of variously substituted aryl bromide and phenyl boronic acid reagents was carried out in the presence of 0.3 mol% Pd/G and potassium carbonate (3 eq.) using H_2O:EtOH (1:1) as environmentally benign solvents. The reactions are either completed at room temperature or heated under microwave irradiation (MWI) at 80 °C for 10 min. In this context, a broad range of aryl bromide containing electron-donating (**1d–e**) and electron-withdrawing groups (**1a–c**) can be effectively incorporated in the coupling products. In addition, phenyl boronic acids bearing useful functionality such as 4-dimethylamino (**1c, g**), 4-amino carbonyl (**1d, f**), or 4-thiomethyl (**1b**) all led to high yield of Suzuki products. We were pleased to find that even a more difficult substrate such as 4-nitro-1-chlorobenzene was able to undergo Suzuki coupling with phenyl boronic acid in good yield (**1h**).

Table 1
Recycling experiments with Pd/G and Pd/GO catalysts using a concentration of 0.3 mol%.[a]

Run	Conversion (%)[b] Pd/G	Conversion (%)[b] Pd/GO
1	100	100
2	100	100
3	100	100
4	100	100
5	100	96
6	98	54
7	98	23
8	96	5
9	62	–
10	28	–
11	8	–

[a] Bromobenzene (50 mg, 0.32 mmol), boronic acid (47 mg, 0.382 mmol, 1.2 eq.), potassium carbonate (133 mg, 0.96 mmol, 3 eq.), and Pd/G (1.3 mg, 0.96 μmol, 0.3 mol%) in 4 mL (H_2O:EtOH) (1:1) were heated at 80 °C (MWI) for 5 min.
[b] Conversions were determined by GC–MS.

3.3. Activity of Pd/G catalyst toward the Heck reaction

To generalize the application of the Pd/G catalyst to another carbon–carbon bond forming process, the evaluation of the catalytic activity of the Pd/G catalyst was extended to the Heck reaction. While Heck reactions typically involve the use of phosphine-based palladium catalysis in homogeneous systems, we chose to examine our heterogeneous Pd/G nanoparticles under ligand-free conditions using microwave irradiation. Thus, the reaction of a diverse range of aryl bromides with a variety of olefins was evaluated using 0.3 mol% of Pd/G, potassium carbonate (3 eq.) and H_2O:EtOH as solvents at the temperature of 180 °C using a microwave irradiation as a heating source. As shown in Table 3, a variety of electron-rich (**2d, g**) and electron-poor (**2c, f**) aryl bromide substrates can easily undergo the Heck coupling with a relatively unactivated alkene such as tert-butylstyrene (**2b, f**), achieving an excellent yield of the Heck products.

3.4. Composition of active catalytic species

The difference in the activity of the Pd/G and Pd/GO catalysts could be attributed to a number of parameters such as the nature

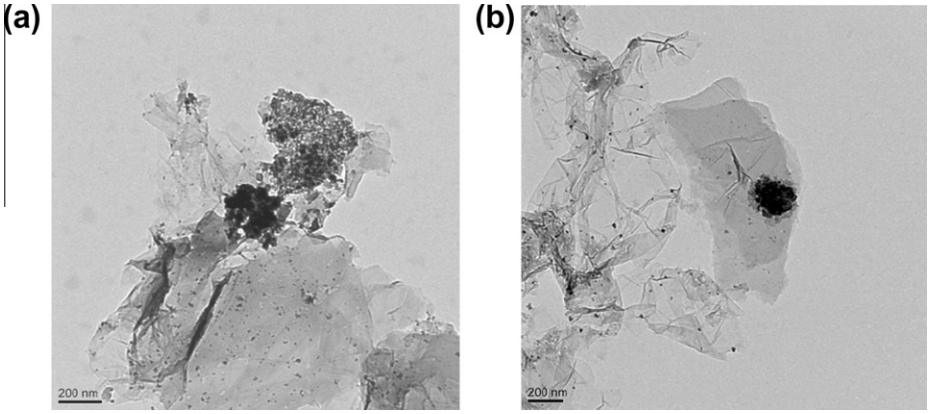

Fig. 7. TEM images of (a) Pd/G after the 10th run and (b) Pd/GO after the 7th run.

Table 2
Evaluation of catalysts for Suzuki cross-coupling.[a]

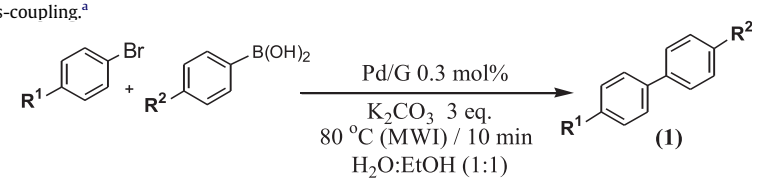

cpd	Aryl halide	Boronic acid	1(%)[c]
a[b]	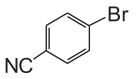	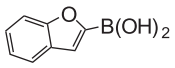	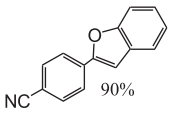 90%
b	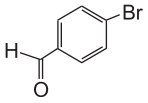	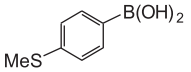	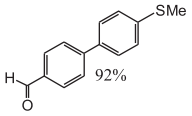 92%
c	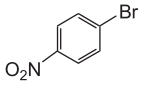	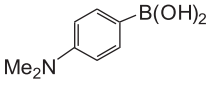	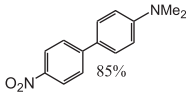 85%
d	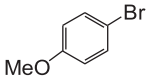	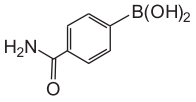	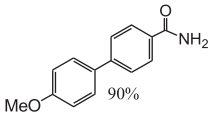 90%
e[b]	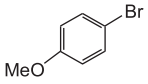	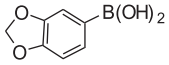	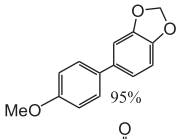 95%
f		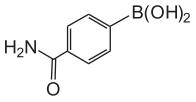	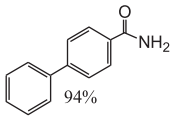 94%
g	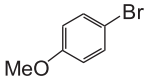	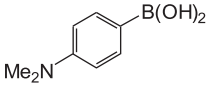	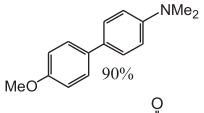 90%
h	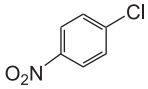	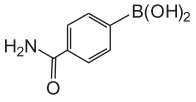	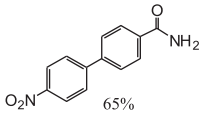 65%

[a] Aryl halide (0.51 mmol), boronic acid (0.61 mmol, 1.2 eq.), potassium carbonate (212 mg, 1.53 mmol, 3 eq.), and Pd/G (2.1 mg, 1.53 μmol, 0.3 mol%) in 8 mL (H_2O:EtOH) (1:1) were heated at 80 °C (MWI) for 10 min.
[b] Reactions were completed at r.t. after 30 min.
[c] Isolated yields.

and concentration of the active species, particle size, dispersion, and surface area. To gain further insight into the nature of the Pd species on the surface of graphene or GO support, we measured the XPS spectra of the Pd/G and Pd/GO catalysts before and after the Suzuki reaction in Scheme 1 at room temperature. The results shown in Fig. 8 indicate the presence of different oxidation states of Pd within the supported catalysts before and after the reaction.

The as-prepared Pd/GO catalyst consists mainly of Pd oxides as evident from the measured binding energies of the Pd $3d^{5/2}$ and $3d^{3/2}$ electrons at 337.8 and 343.2 eV, respectively corresponding to Pd(II). However, during the cross-coupling reaction, *in situ* reduction to Pd(0) occurs most likely by the solvent under basic conditions. The *in situ* reduction of Pd(II) is confirmed by the measured binding energies of the Pd $3d^{5/2}$ and $3d^{3/2}$ electrons after the reaction at 335.7 and 341 eV, respectively, thus corresponding to a mixture of Pd oxides and Pd(0) species. On the other hand, for the as-prepared Pd/G catalyst, part of the Pd(II) is already reduced to Pd(0) during the preparation of the catalyst by the HH reduction of the GO-Pd nitrate mixture under MWI. This is clearly illustrated in Fig. 8 by the almost identical XPS spectra of the Pd/GO catalyst after the reaction and the Pd/G catalyst before the reaction. Following the cross-coupling reaction, *in situ* reduction of the remaining Pd(II) species in the Pd/G catalyst converts the catalyst to mostly Pd(0) species, which are the active species in Pd-catalyzed cross-coupling reactions. The remarkable activity and recyclability of the Pd/G catalyst appears to be clearly related to the high concentration of Pd(0) species already present in the as-prepared catalyst in contrast to the Pd/GO in which palladium reduction occurs *in situ* during the reaction. It would be interesting to systematically examine the effect of increasing the concentration of the Pd(0) in the Pd/G catalyst on the catalytic activity. For this purpose, the catalytic activities of different Pd/G catalysts with similar particle size but different concentrations of Pd(0) should be compared. This work is currently in progress in our laboratory, and the results will be reported elsewhere [64].

We attribute the great reactivity of the Pd/G catalysts prepared by MWI to the small size of the Pd nanoparticles (7–9 nm), the high degree of dispersion due to the lack of evidence for agglomeration of the nanoparticles during the preparation, and the high concentration of the Pd(0) species already present in the as-prepared

Table 3
Evaluation of catalysts for Heck reactions.[a]

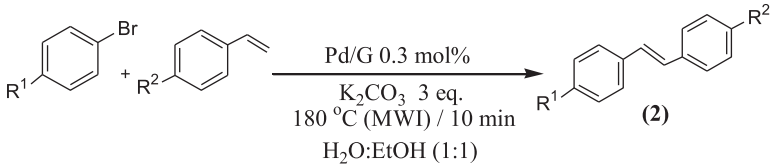

cpd	Aryl bromide	Olefin	2(%)[b]
a	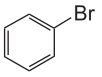	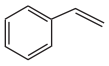	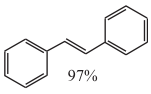 97%
b	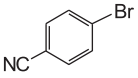	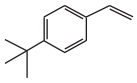	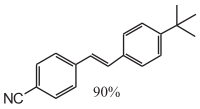 90%
c	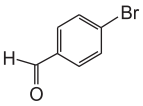	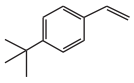	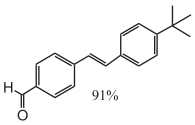 91%
d	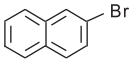	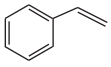	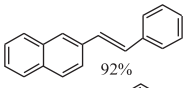 92%
e	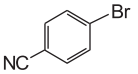	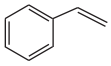	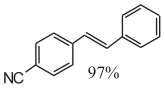 97%
f	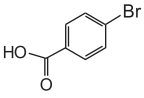	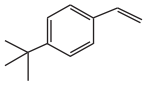	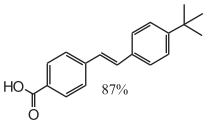 87%
g	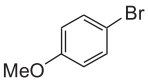	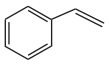	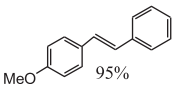 95%
h	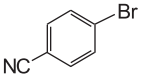	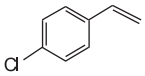	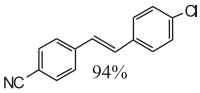 94%
i	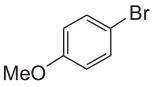	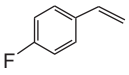	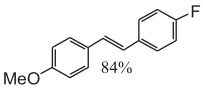 84%

[a] Aryl bromide (0.51 mmol), alkene (1.02 mmol, 2 eq.), potassium carbonate (212 mg, 1.53 mmol, 3 eq.), Pd/G (2.1 mg, 1.53 μmol, 0.3 mol%) in 8 mL (H_2O:EtOH) (1:1) were heated at 180 °C (MWI) for 10 min.
[b] Isolated yields.

catalyst (XPS results, Fig. 8). It is noteworthy that the palladium nitrate source used for catalyst preparation has excellent solubility in water, and there is no concern regarding the possibility of precipitating the palladium nitrate on GO. Furthermore, the current MWI procedure is a very effective technique for simultaneous reduction of both the Pd ions (from palladium nitrate) and GO using HH, providing a rapid temperature rise during microwave heating in water, thus leading to a fast nucleation and consequently small uniform Pd nanoparticles (7–9 nm) well dispersed on the resulting graphene sheets (TEM results, Fig. 4a). It should be noted that the simultaneous reduction of GO and the Pd ions in solution followed by the heterogeneous nucleation of Pd nanoparticles on the large surface area of graphene is the most important and unique feature of our MWI synthesis approach of the highly active Pd/G catalyst. We have previously demonstrated that simple physical mixing of separately prepared very small Pd nanoparticles (4–6 nm) and reduced GO sheets results in significant aggregation of the Pd nanoparticles with very poor dispersion on the graphene sheets [28]. On the other hand, the simultaneous reduction of the Pd ions with GO results in well-dispersed nanoparticles on the graphene sheets, thus suggesting that specific interaction between the Pd nanocrystals and the graphene sheets may be responsible for dispersion of the nanoparticles. This is also consistent with the enhanced thermal stability of the Pd/G over the graphene sheets as shown in Fig. 5. Furthermore, our results indicate that the simultaneous reduction of GO and the Pd ions results in a higher concentration of the catalytically active Pd(0) in the as-prepared catalyst which enhances the nearly dominant heterogeneous nature of the catalytic reaction system. Therefore, the current work clearly demonstrates that the catalyst preparation method exerts the major influence in determining the properties and hence the activity of the catalyst. In addition, the significance of graphene as an ideal support system for palladium can also be attributed to its remarkable structural and electronic features. The unique hexagonal planar structure of the graphene and the presence of C=C bonds within the graphene matrix may play an important role as an electron-rich labile support system for palladium, which stabilizes the metal center, prevents deactivation of the catalyst by agglomeration, and increases the catalytic activity of the palladium nanoparticles for cross-coupling reactions.

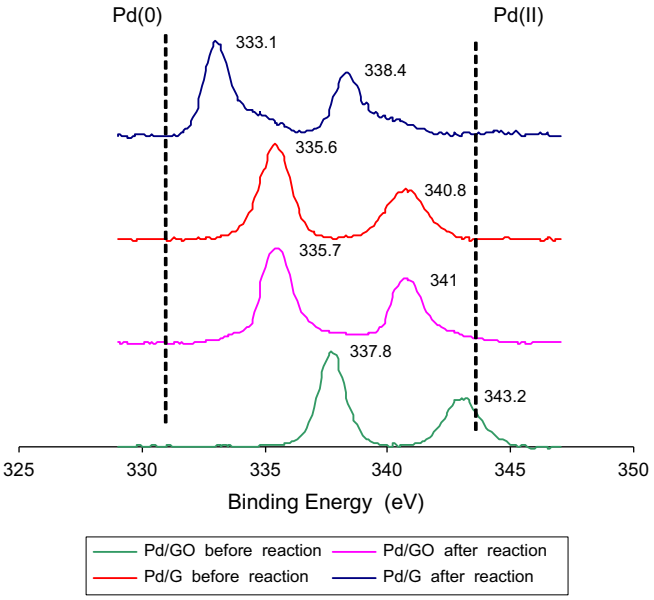

Fig. 8. XPS spectra of the Pd $3d^{5/2}$ and $3d^{3/2}$ electrons' binding energies for Pd/G and Pd/GO catalysts before and after Suzuki reactions (Scheme 1).

4. Conclusions

In conclusion, we have developed an efficient method to generate highly active Pd nanoparticles supported on graphene by microwave-assisted chemical reduction of the corresponding aqueous mixture of palladium nitrate and dispersed graphite oxide sheets. These catalysts offer a number of advantages such as high stability of the catalyst, easy removal from the reaction mixture, reusability of the catalyst for eight times with minimal loss of activity, and significantly better performance than the well-known commercial Pd/C catalyst. Both Pd/G and Pd/GO demonstrated excellent catalytic activity for the carbon–carbon cross-coupling reactions under ligand-free ambient conditions in an environmentally friendly solvent system. However, the Pd/G containing 7.9 wt.% palladium demonstrated a remarkable turnover frequency (108,000 h^{-1}) in the Suzuki cross-coupling reactions using MWI heating conditions. We also found strong evidence that the outstanding reactivity and recyclability of the Pd/G catalyst toward Suzuki cross-coupling reactions is associated with high concentration of Pd(0) nanoparticles very well dispersed on the surface of the graphene sheets. This catalyst also demonstrated a broad range of utility for Heck coupling reactions.

Acknowledgments

We thank NSF (CHE-0911146) and (CHE-0820945) for the support of this work. We gratefully acknowledge Prof. Jim Terner (VCU) for the Raman measurements, Prof. Maryanne Collinson (VCU) for the AFM measurements, and Dr. Dmitry Pestov for the XPS analyses.

Appendix A. Supplementary material

Complete NMR and mass spectrometric data of the reaction products; EDS, XPS, TEM, and AFM data of graphene samples prepared by the HH-MWI method. Supplementary data associated with this article can be found, in the online version, at doi:10.1016/j.jcat.2010.12.003.

References

[1] A.K. Geim, Science 324 (2009) 1530.
[2] A.K. Geim, Nat. Mater. 6 (2007) 183.
[3] K.S. Novoselov, A.K. Geim, S.V. Morozov, D. Jiang, M.L. Katsnelson, I.V. Grigorieva, S.V. Dubonos, A.A. Firsov, Nature 438 (2005) 197.
[4] K.S. Novoselov, A. K Geim, S.V. Morozov, D. Jiang, Y. Zhang, S.V. Dubonos, I.V. Grigorieva, A.A. Firsov, Science 306 (2004) 666.
[5] M.J. Allen, V.C. Tung, R.B. Kaner, Chem. Rev. 110 (2009) 132.
[6] C.N.R. Rao, A.K. Sood, K.S. Subrahmanyam, A. Govindaraj, Angew. Chem. Int. Ed. 48 (2009) 7752.
[7] J. Wu, W. Pisula, K. Müllen, Chem. Rev. 107 (2007) 718.
[8] S. Stankovich, D.A. Dikin, G.H.B. Dommett, K.M. Kohlhaas, E.J. Zimney, E.A. Stach, R.D. Piner, S.T. Nguyen, R.S. Ruoff, Nature 442 (2006) 282.
[9] S. Watcharotone, D.A. Dikin, S. Stankovich, R. Piner, I. Jung, G.H.B. Dommett, G. Evmenenko, S.E. Wu, S.F. Chen, C.P. Liu, S.T. Nguyen, R.S. Ruoff, Nano Lett. 7 (2007) 1888.
[10] G. Eda, G. Fanchini, M. Chhowalla, Nat. Nanotechnol. 3 (2008) 270.
[11] V.C. Tung, M.J. Allen, Y. Yang, R.B. Kaner, Nat. Nanotechnol. 4 (2009) 25.
[12] P.V.J. Kamat, Phys. Chem. Lett. 1 (2010) 520.
[13] B. Seger, P.V. Kamat, J. Phys. Chem. C 113 (2009) 7990.
[14] G. Williams, B. Seger, P.V. Kamat, ACS Nano 2 (2008) 1487.
[15] Y.C. Si, E.T. Samulski, Chem. Mater. 20 (2008) 6792.
[16] C. Xu, X. Wang, J.W. Zhu, J. Phys. Chem. C 112 (2008) 19841.
[17] R. Muszynski, B. Seger, P.V. Kamat, J. Phys. Chem. C 112 (2008) 5263.
[18] G. Goncalves, P.A.A.P. Marques, C.M. Granadeiro, H.I.S. Nogueira, M.K. Singh, J. Gracio, Chem. Mater. 21 (2009) 4796.
[19] X. Zhou, X. Huang, X. Qi, S. Wu, C. Xue, F.Y.C. Boey, Q. Yan, P. Chen, H. Zhang, J. Phys. Chem. C 113 (2009) 10842.
[20] Y.H. Lu, M. Zhou, C. Zhang, Y.P. Feng, J. Phys. Chem. C 113 (2009) 20156.
[21] K.S. Novoselov, Z. Jiang, Y. Zhang, S.V. Morozov, H.L. Stormer, U. Zeitler, J.C. Maan, G.S. Boebinger, P. Kim, A.K. Geim, Science 315 (2007) 1379.
[22] C. Gomez-Navarro, M. Burghard, K. Kern, Nano Lett. 8 (2008) 2045.
[23] Z. Luo, L.A. Somers, Y. Dan, T. Ly, N.J. Kybert, E.J. Mele, A.T. Charlie Johnson, Nano Lett. 10 (2010) 777.
[24] S. Park, R.S. Ruoff, Nat. Nanotechnol. 4 (2009) 217.
[25] S. Stankovich, R.D. Piner, X. Chen, N. Wu, S.T. Nguyen, R.S. Ruoff, J. Mater. Chem. 16 (2006) 155.
[26] S. Stankovich, D.A. Dikin, R.D. Piner, K.M. Kohlhaas, A. Kleinhammes, Y. Jia, Y. Wu, S.T. Nguyen, R.S. Ruoff, Carbon 45 (2007) 1558.
[27] S. Park, J. An, I. Jung, R.D. Piner, S.J. An, X. Li, A. Velamakanni, R.S. Ruoff, Nano Lett. 9 (2009) 1593.
[28] H.M.A. Hassan, V. Abdelsayed, A.E.R. Khder, K.M. AbouZeid, J. Terner, M.S. El-Shall, S.I. Al-Resayes, A. El-Azhary, J. Mater. Chem. 19 (2009) 3832.
[29] S.L. Buchwald, Acc. Chem. Res. 41 (2008) 1439.
[30] L. Yin, J. Liebscher, Chem. Rev. 107 (2007) 133.
[31] R.F. Heck, Acc. Chem. Res. 12 (1979) 146.
[32] N. Miyaura, A. Suzuki, Chem. Rev. 95 (1995) 2457.
[33] I.P. Beletskaya, A.V. Cheprakov, Chem. Rev. 100 (2000) 3009.
[34] C.J. Welch, J. Albaneze-Walker, W.R. Leonard, M. Biba, J. DaSilva, D. Henderson, B.B. Laing, D.J. Mathre, S. Spencer, X. Bu, T. Wang, Org. Process Res. Dev. 9 (2005) 198.
[35] C.E. Garrett, K. Prasad, Adv. Synth. Catal. 346 (2004) 889.
[36] B.M. Bhanage, M. Arai, Catal. Rev. 43 (2001) 315.
[37] K. Köhler, R.G. Heidenreich, S.S. Soomro, S.S. Pröckl, Adv. Synth. Catal. 350 (2008) 2930.
[38] L. Djakovitch, K. Koehler, J. Am. Chem. Soc. 123 (2001) 5990.
[39] L. Djakovitch, K. Koehler, J. Mol. Catal. A: Chem. 142 (1999) 275.
[40] J. Li, A.W.H. Mau, C.R. Strauss, Chem. Commun. (1997) 1275.
[41] H. Erdoğan, Ö. Metin, S. Özkar, Phys. Chem. Chem. Phys. 11 (2009) 10519.
[42] R. Narayanan, M. El-Sayed, J. Am. Chem. Soc. 125 (2003) 8340.
[43] R. Narayanan, M. El-Sayed, J. Phys. Chem. B 108 (2004) 8572.
[44] C. Duanmu, I. Saha, Y. Zheng, B.M. Goodson, Y. Gao, Chem. Mater. 18 (2006) 5973.
[45] R. Narayanan, M. Tabor, M. El-Sayed, Top. Catal. 48 (2008) 60.
[46] P.J. Ellis, I.J.S. Fairlamb, S.F.J. Hackett, K. Wilson, A.F. Lee, Angew. Chem. Int. Ed. 49 (2010) 1820.
[47] S. Wittmann, A. Schatz, R.N. Grass, W.J. Stark, O. Reiser, Angew. Chem. Int. Ed. 49 (2010) 1867.
[48] M. Irfan, M. Fuchs, T.N. Glasnov, C.O. Kappe, Chem. Eur. J. 15 (2009) 11608.
[49] G.M. Scheuermann, L. Rumi, P. Steurer, W. Bannwarth, R. Mülhaupt, J. Am. Chem. Soc. 131 (2009) 8262.
[50] J.A. Gerbec, D. Magana, A. Washington, G.F. Strouse, J. Am. Chem. Soc. 127 (2005) 15791.
[51] A.B. Panda, G.P. Glaspell, M.S. El-Shall, J. Am. Chem. Soc. 128 (2006) 2790.
[52] A.B. Panda, G.P. Glaspell, M.S. El-Shall, J. Phys. Chem. C 111 (2007) 1861.
[53] V. Abdelsayed, A.B. Panda, G.P. Glaspell, M.S. El-Shall, in: R. Nagarajan, T. Alan Hatton, (Eds.), Nanoparticles: Synthesis, Stabilization, Passivation, and Functionalization, ACS Symposium Series, 2008, p. 996 (Chapter).
[54] V. Abdelsayed, A. Aljarash, M.S. El-Shall, Z.A. Al Othman, A.H. Alghamdi, Chem. Mater. 21 (2009) 2825.
[55] M. Larhed, C. Moberg, A. Hallberg, Acc. Chem. Res. 35 (2002) 717.
[56] W.S. Hummers Jr., R.E. Offeman, J. Am. Chem. Soc. 80 (1958) 1339.
[57] A.C. Ferrari, Solid State Commun. 446 (2007) 60.
[58] S. Berciaud, S. Ryu, L.E. Brus, T.F. Heinz, Nano Lett. 9 (2009) 346.

[59] M.S. Dresselhaus, A. Jorio, M. Hofmann, G. Dresselhaus, R. Saito, Nano Lett. 10 (2010) 751.
[60] I.W. Davies, L. Matty, D.L. Hughes, P.J. Reider, J. Am. Chem. Soc. 123 (2001) 10139.
[61] K. Köhler, R.G. Heidenreich, J.G.E. Krauter, J. Pietsch, Chem. Eur. J. 8 (2002) 622.
[62] N.E. Leadbeater, V.A. Williams, T.M. Barnard, M.J. Collins, It was demonstrated that ultra-low amounts of Pd loading can effectively catalyze the Suzuki and Heck coupling reactions, Org. Process Res. Dev. 10 (2006) 833.
[63] R.K. Arvela, N.E. Leadbeater, J. Org. Chem. 70 (2005) 1786.
[64] N. Herring, A.R. Siamaki, S. Moussa, F. Gupton, M.S. El-Shall, in preparation.